

MATRIX-FIBER INTERFACE CHARACTERIZATION IN METAL MATRIX COMPOSITES USING ULTRASONIC SHEAR-WAVE BACK-REFLECTION COEFFICIENT TECHNIQUE

Theodore E. Matikas
National Research Council Fellow
NDE Branch, Materials Directorate, WL/MLLP
Wright-Patterson Air Force Base, OH 45433-6533

Prasanna Karpur
Research Institute, University of Dayton
300 College Park Avenue
Dayton OH 45469-0127

INTRODUCTION

There are several methods to characterize the interfacial strength between matrix and fiber in metal matrix composites: destructively, using "push-out" tests, or the "fiber fragmentation" technique, by subjecting a single fiber sample (made by diffusion bonding of two matrix plates) to axial loading and by measuring the size of fragments that is linked to the "load transfer behavior". The critical length of fiber for load transfer is a function of the interfacial shear stress [1]. Recently, ultrasonic imaging of the fiber fragmentation [2], in conjunction with advanced signal processing techniques [3], was performed by the authors.

The objective of this work is to evaluate the interfacial properties of continuous fiber reinforced metal matrix composites using another NDE (ultrasonic) method: by using shear interrogation and by measuring the back-reflection signal from the fibers (ultrasonic beam is obliquely incident to the sample and in a plane normal to the axis of the fibers).

In order to define the conditions for that technique, we present in this paper a theoretical modeling of the reflection of an ultrasonic beam from a single fiber embedded in a metal matrix. We discuss the dependence of the back-reflection coefficient and of the resonance dips of the composite system on the interfacial stiffness between the matrix and the fiber.

In this study, two model monofilament titanium based composites (SCS-6 SiC fiber reinforced Ti-6Al-4V (by weight) and Ti-24Al-11Nb (Ti-14Al-21Nb by weight)) have been analytically modeled for reflectivity analysis.

MODEL

A nondestructive ultrasonic test consists of using the incident wave to excite the matrix/fiber interface. The interface between the two media, will transmit part of the energy into the fiber and will reflect another part of the wave. Here, it is assumed that the vibration is

Case (a) First, let us consider an ultrasonic beam incident on the fluid-composite interface. The transmission coefficient for a shear wave propagating in the matrix is given by:

$$T_S = -2 \frac{\left(\frac{c_{2S}}{c_{2L}}\right)^2 \sin 2\theta_{2L}}{\left(\frac{c_{2S}}{c_{2L}}\right)^2 \sin 2\theta_{2L} \sin 2\theta_{2S} + \cos^2 2\theta_{2S} + \frac{\rho_1 c_1}{\rho_2 c_{2L}} \frac{\cos \theta_{2L}}{\cos \theta}} \quad (1)$$

Case (b) Let us now consider an acoustic plane wave of displacement amplitude A_{2n} propagating in the positive direction of the z' axis and normally incident to the matrix-fiber interface (Fig. 1). The fiber, and the upper and lower regions of the matrix are denoted by medium 3, medium 2 and medium 4 respectively. The two interfaces between matrix and fiber are normal to the z' axis with 'upper' interface located within the plane $z'=d$ (interface A) and 'lower' interface within the plane $z'=d+d'$ (interface B). In medium 2, two waves are propagating: one incident to the interface $z'=d$ and one reflected from that interface. In medium 3, also two waves are propagating: one incident to the interface $z'=d+d'$ and one reflected from that interface. In medium 4, we must consider only one wave (the transmitted wave). Medium 4 can be considered as semi-infinite; no part of the wave of amplitude A_{4n} is re-transmitted to medium 3 according to the configuration of figure 1.

The displacements (in the directions of z' axis) in the media 2, 3, and 4, are given by the expressions

$$\begin{aligned} u_{2n} &= A_{2n} \exp[i(\omega t + k_{2n} z')] + A_{2n}^R \exp[i(\omega t - k_{2n} z')] \\ u_{3n} &= A_{3n} \exp[i(\omega t + k_{3n} z')] + A_{3n}^R \exp[i(\omega t - k_{3n} z')] \\ u_{4n} &= A_{4n} \exp[i(\omega t + k_{2n} z')] \end{aligned} \quad (2)$$

and are subsequently related to the stresses by the equations

$$\begin{aligned} \sigma_{2n} &= i Z_{2n} c_{2n} k_{2n} \{ A_{2n} \exp[i(\omega t + k_{2n} z')] - A_{2n}^R \exp[i(\omega t - k_{2n} z')] \} \\ \sigma_{3n} &= i Z_{3n} c_{3n} k_{3n} \{ A_{3n} \exp[i(\omega t + k_{3n} z')] - A_{3n}^R \exp[i(\omega t - k_{3n} z')] \} \\ \sigma_{4n} &= i Z_{2n} c_{2n} k_{2n} \{ A_{4n} \exp[i(\omega t + k_{2n} z')] \} \end{aligned} \quad (3)$$

where the numbers in the subscripts denote the medium with which the quantity is associated.

The Interface Conditions Between Matrix and Fiber

The debonding between matrix and fiber is modeled by: (1) assuming continuity of normal and shear stresses and normal displacements at the interface, (2) allowing the discontinuity of shear displacements at the interface (tangential 'elastic' slip which is proportional to shear traction, and characterized by a newly proposed positive coefficient N_n). In general, the interfacial stiffness of the two matrix-fiber boundaries (upper and lower) can be different, due to the fabrication conditions (different bonding between the fiber and the upper or lower matrix plate) or due to the use of different material for each matrix plate. Thus, for generality we have to consider different coefficients N_n and \tilde{N}_n for each interface.

Accordingly, the interface conditions are

$$[u^P] = 0, \quad [\sigma^P] = 0, \text{ and } [\sigma^T] = 0 \quad (4)$$

$$\sigma^T = N_n [u^T] \quad (\text{interface } z' = d) \quad \text{or} \quad \tilde{\sigma}^T = \tilde{N}_n [u^T] \quad (\text{interface } z' = d + d')$$

where the superscripts P and T denote normal displacements or stresses and tangential displacements or shear tractions respectively, and where the square brackets denote the jump of a function across the interface, with

$$u^P = u \cdot m \quad \sigma^P = \sigma_{ij} m_i m_j \quad u^T = u - u^P \cdot m \quad \sigma^T = \sigma - \sigma^P \cdot m \quad (5)$$

where m is the outward unit normal to medium 3 and u and σ denote the displacement and traction vectors at the interface.

With the assumption of instantaneously transmitted stress through the springs from medium 2 to medium 3 and from 3 to 4, the pressure reflection coefficient $W_n = A_{2n}^R / A_{2n}$ can be derived from the systems of equations (2)-(4):

$$W_n = \frac{Q1_n - Q2_n}{Q3_n - Q4_n} e_n \quad (6)$$

where $Q1_n$, $Q2_n$, $Q3_n$ and $Q4_n$ are complex quantities expressed by the equations:

$$\begin{aligned} Q1_n &= X_n^2 Y_n^2 (e_n' - 1) + N_n \tilde{N}_n (X_n^2 - Y_n^2) (1 - e_n') \\ Q2_n &= X_n Y_n \{ \tilde{N}_n [X_n (1 + e_n') + Y_n (1 - e_n')] + N_n [X_n (1 + e_n') - Y_n (1 - e_n')] \} \\ Q3_n &= X_n^2 Y_n^2 (e_n' - 1) + N_n \tilde{N}_n [(X_n^2 + Y_n^2) (1 - e_n') + 2 X_n Y_n (1 + e_n')] \\ Q4_n &= X_n Y_n \{ \tilde{N}_n [X_n (1 + e_n') + Y_n (1 - e_n')] + N_n [X_n (1 + e_n') + Y_n (1 - e_n')] \} \end{aligned} \quad (7)$$

with

$$\begin{aligned} X_n &= Z_{2n} c_{2n} k_{2n} = 2\pi \rho_2 c_{2n} f & Y_n &= Z_{3n} c_{3n} k_{3n} = 2\pi \rho_3 c_{3n} f \\ e_n' &= \exp [i k_{3n} 2d'] & e_n &= \exp [i k_{2n} 2d] \end{aligned} \quad (8)$$

Note that, the case of infinitely rigid springs ($N_n, \tilde{N}_n \rightarrow \infty$) corresponds to perfect interfaces, and the coefficient W_n is given by the simplified expression

$$W_n = \frac{(X_n^2 - Y_n^2) (1 - e')}{(X_n^2 + Y_n^2) (1 - e') + 2 X_n Y_n (1 + e')} \quad (9)$$

whereas, the case of infinitely compliant springs ($N_n, \tilde{N}_n = 0$) corresponds to complete

unbond; in that case, the boundary of the matrix becomes free surface and no energy is transmitted into the fiber. The magnitude of the reflection coefficient (13) becomes

$$|W_n| = 1 \quad (\text{even if } \tilde{N}_n \rightarrow \infty) \quad (10)$$

representing total reflection from the fiber. As a result, this model allows for bonding between $N_n=0$ and $N_n=\infty$ representing different degrees of chemical / mechanical bonding. Such 'degree of chemical / mechanical bonding' has been shown to exist by metallography in [2].

In reality, we have never those extreme situations: the existence of residual stresses due to the mismatch of the thermal expansion coefficient provides a lower limit to the interface stiffness N_{\min} , whereas the properties of the two materials in contact together with the sensitivity limitation of the ultrasonic technique provide an upper limit to the interface stiffness N_{\max} .

Case (c) Finally, we consider the shear displacement wave of amplitude A_{2n}^R to be incident at the interface between media 2 and 1. The corresponding transmission coefficient is then given by

$$TF_S = \frac{2}{M} \frac{\rho_1 c_1}{\rho_2 c_{2L}} \frac{\cos \theta_{2L} \sin 2\theta_{2S}}{\cos \theta} \quad (11)$$

Thus, the back-reflection coefficient from the fiber is given by:

$$R_S = T_S W_S TF_S \quad (12)$$

and depends on the:

- properties of the matrix (density, ρ_2 , longitudinal, c_{2L} , and shear, c_{2S} , velocities)
- properties of the fiber (density, ρ_3 , longitudinal, c_{3L} , and shear, c_{3S} , velocities)
- diameter of the fiber, d'
- angle of incidence, θ
- frequency, f
- interfacial stiffness, N_n

NUMERICAL AND EXPERIMENTAL RESULTS

The back-reflection coefficient amplitude as a function of interfacial stiffness and frequency for a Ti-6Al-4V/SCS-6 composite is shown in figure 2a. In the range of frequencies of 10-50 MHz we observe two resonance peaks, at 19MHz and 42MHz, and a dip, at 27MHz. Figure 2b (contour map representation) shows that the frequency of the resonance dip and peaks is shifted up followed by a downshift as the stiffness increases from 0 (complete unbond) to 20 (almost perfect bond). This shift would be equivalent to a nonlinear variation in the effective cross-sectional area occupied by the fiber. Figure 3 shows the frequency of the resonance dip from 27MHz for a value of stiffness 0.5, shifted to 30MHz for stiffness 2.5 and downshifted to 29MHz and 26.5MHz for stiffness 6.5 and 20 respectively.

The use of appropriate frequency is an important parameter in order to improve the sensitivity of the technique. Figure 4 shows that frequencies before a resonance dip (24MHz) (Fig. 4b) give better dynamic range than frequencies near a peak (50MHz) (Fig.4d). At 11MHz (Fig.4a), the back-reflection ultrasonic signal has about the same amplitude from stiffness 2 and higher. Also, it is important to chose frequencies where the dependence of the

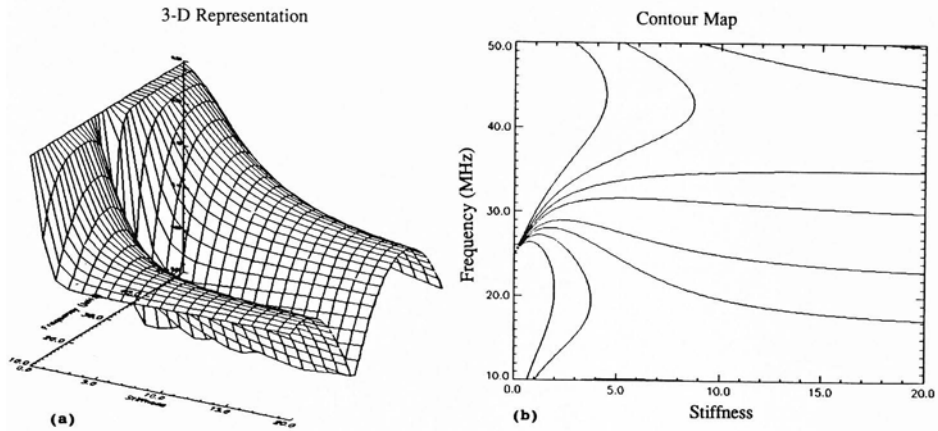


Fig. 2 Ti-6Al-4V/SCS-6: Reflectivity as a function of Stiffness and Frequency.

reflectivity on the stiffness is a monotonic function. Otherwise, a situation shown in fig. 4c will result wherein, for a frequency of 27MHz the same amplitude of signal corresponds to various interfacial conditions

For a given composite system the interfacial stiffness has a minimum and a maximum value, as discussed before, and hence a range of potential values can be defined. In a realistic composite, the manufacturing conditions (temperature, pressure, etc.) influence the interfacial properties thereby causing the value of stiffness to be within this range. Hence, within the same composite system, the main goal of the reflectivity analysis is to monitor the interfacial stiffness to be used as a tool for process control of the manufacturing of composites.

Figure 5 shows theoretical curves of the back-reflection amplitude vs. stiffness for two different composite systems. We can observe that for a given value of stiffness the back-reflection amplitude for Ti-6Al-4V/SCS-6 is greater than for Ti-24Al-11Nb/SCS-6. However, when six different samples (three of each composite system) were used for reflectivity analysis, all the measurements show clearly that the relative back-reflection amplitude from a Ti-24Al-11Nb/SCS-6 is greater than the back-reflection amplitude from a Ti-6Al-4V/SCS-6 (see table in figure 5). Therefore, it is logical to argue that the difference in the interfacial stiffness coefficient is causing such an 'apparent contradiction' of theoretical and experimental results. This is obvious from Fig. 5 wherein the dotted lines show one of possible combinations of interfacial stiffness which will result in 'apparent contradiction'. As a result, it is deduced that the interface bonding in Ti-24Al-11Nb/SCS-6 is poorer than that of Ti-6Al-4V/SCS-6. Such a hypothesis is corroborated by fiber fragmentation tests, ultrasonic imaging of the fiber fragmentation and metallography [2].

CONCLUSION

A theoretical model has been developed for the characterization of fiber/matrix interfacial strength in composites using shear wave back-reflection coefficient interrogation. The model was used to define the optimum experimental parameters such as frequency of interrogation and angle of incidence.

Preliminary experimentally measured back-reflection data for two different metal matrix composites corroborate with other destructive (fiber fragmentation, metallography) and nondestructive (ultrasonic imaging of the fiber fragmentation) techniques presented in a companion paper [2].

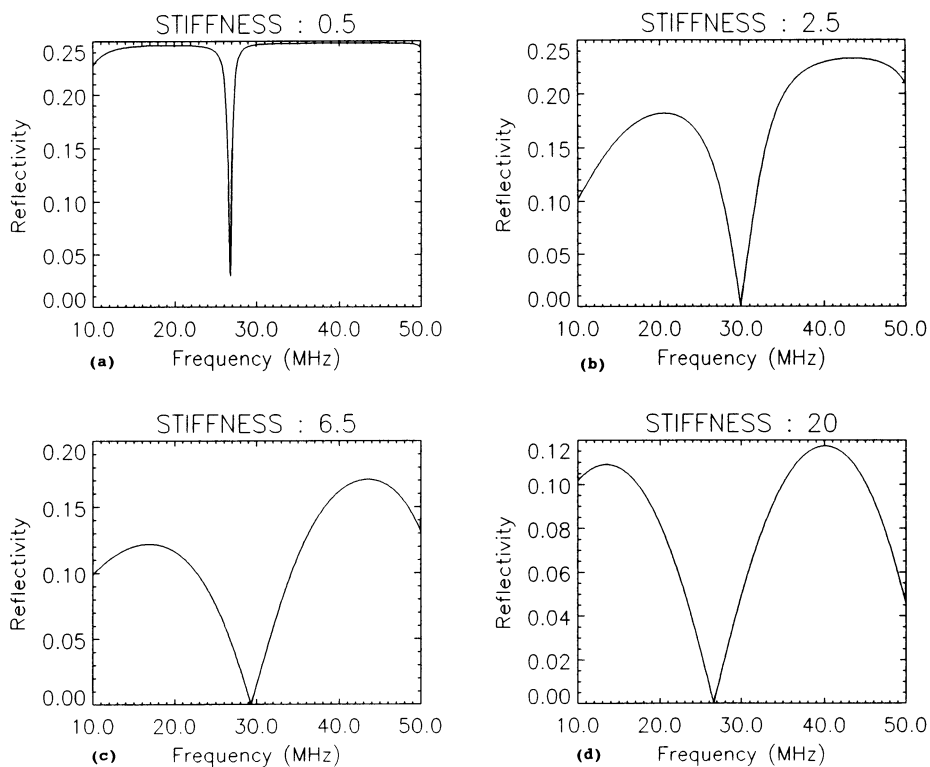


Fig. 3 Back-reflection coefficient. Dependence on Frequency.

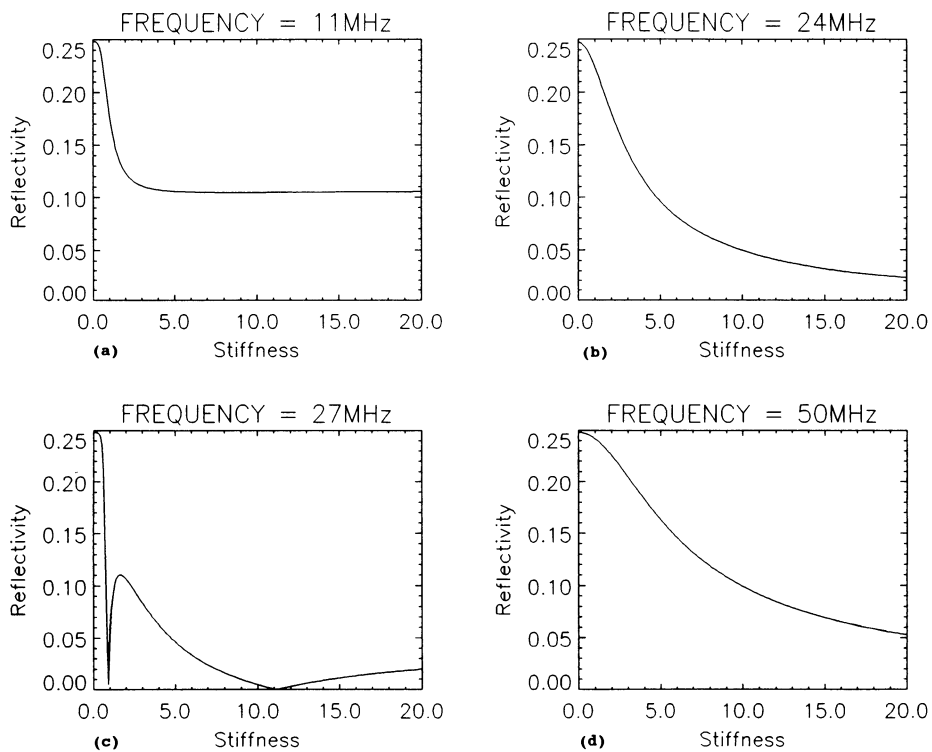


Fig. 4 Back-reflection coefficient. Dependence on Stiffness.

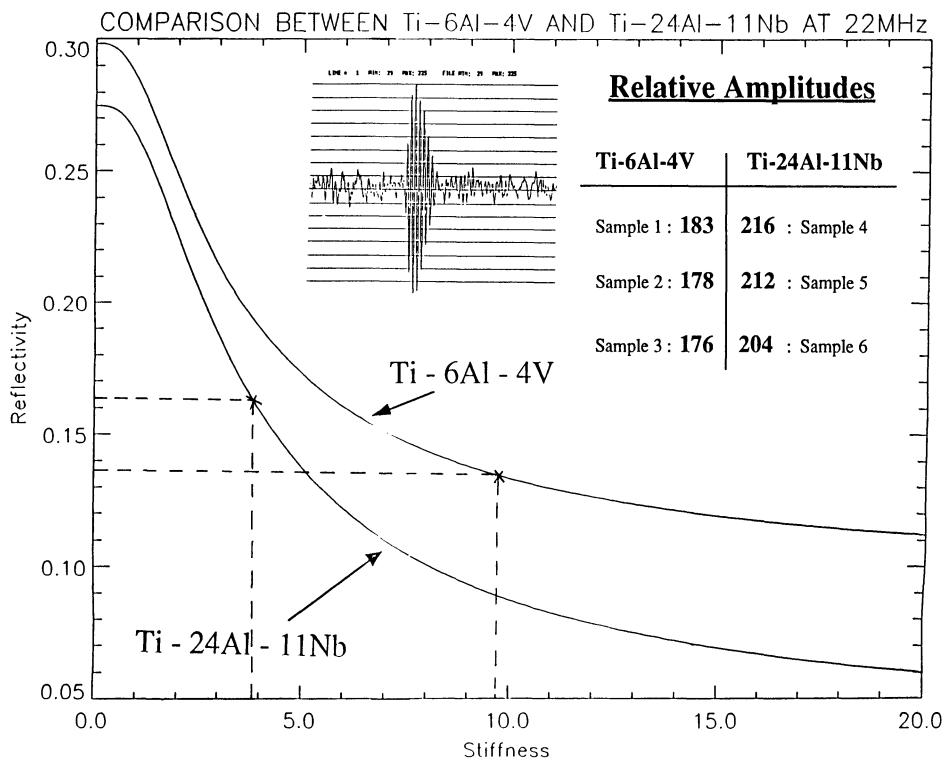


Fig. 5 Back-reflection amplitude vs. Stiffness. Comparison between two composites.

REFERENCES

1. A. Kelly and W.R. Tyson, "Tensile properties of fiber-reinforced metals: Cu-W and Cu-Mo", J. Mech. Phys. Solids, 13 (1965) pp. 329-350.
2. P. Karpur, T. E. Matikas, and S.Krishnamurthy and N.E.Ashbaugh, "Ultrasound for fiber fragmentation size determination to characterize load transfer behavior of matrix-fiber interface in metal matrix composites", in Review in Progress in QNDE, July 19-24, 1992, La Jolla, California.
3. L. Mann, T.E. Matikas, P. Karpur, S.Krishnamurthy, "Supervised backpropagation neural networks for the classification of ultrasonic signals from fiber microcracking in metal matrix composites", 1992 IEEE Ultrasonics Symposium, Tucson, Arizona.